

28<sup>th</sup> October 2021

**Note added after first publication:** This Supplementary Information file replaces that originally published 24<sup>th</sup> July 2020

**Supporting Information for: Imaging and Spectroscopy of Domains of the Cellular Membrane by Photothermal-Induced Resonance.**

Luca Quaroni

*Department of Physical Chemistry and Electrochemistry, Faculty of Chemistry, Jagiellonian University, 30-387, Kraków, Poland*

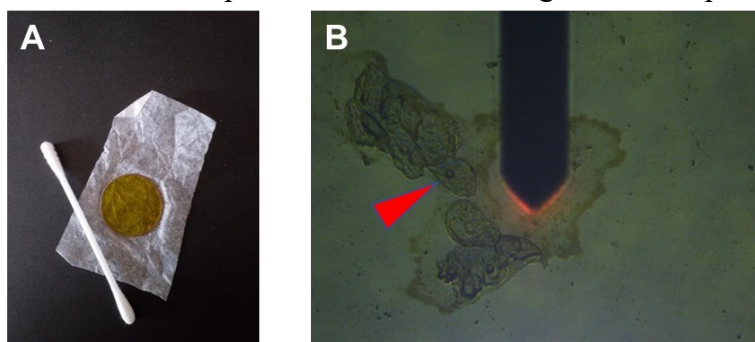
*Institute of Nuclear Physics, Polish Academy of Sciences, 31-342 Kraków, Poland*

**Index**

<i>S1. Preparation of epithelial buccal cells</i>	<i>Page S1</i>
<i>S2. Spatial resolution in conventional PTIR.</i>	<i>Page S1</i>
<i>S3. Depth response in conventional PTIR.</i>	<i>Page S2</i>
<i>S4. Photothermal temperature increase.</i>	<i>Page S2</i>
<i>S5. Comparison of spectra</i>	<i>Page S4</i>
<i>S6. References for Supporting Information</i>	<i>Page S4</i>

*S1. Preparation of Epithelial Buccal Cells*

Supporting Figure S1 shows the tool used for sample collection of epithelial buccal cells (Figure S1A). It also shows the appearance of a buccal cell sample deposited on an IR optical window when inspected with the visible light microscope objective of the PTIR instrument.



*Supporting Figure S1. Sample preparation for PTIR of buccal cells. A. Cotton-tipped stick for cheek swab and optical window to collect cells. B. Visible light image of a cluster of cheek cells in the PTIR sample compartment, ready for measurement. The dark beam is the cantilever of the AFM/PTIR probe. The red glow by the tip is caused by the AFM monitor laser. The red arrow points at the cell measured in Figure 2 of the main text.*

## *S2. Spatial Resolution in Conventional PTIR.*

Previous work has characterized the spatial resolution in the XY plane for spectromicroscopy PTIR measurements in resonant-mode.<sup>1</sup> In the present section we measure the XY spectromicroscopy spatial resolution for conventional PTIR, with excitation removed from a resonant frequency of the cantilever.

### *S2.1 Experimental Procedure and Result*

The sample used for resolution measurements has already been described.<sup>1</sup> It is a 150 nm thick section of PMMA beads, 3  $\mu\text{m}$  in diameter, embedded in an epoxy matrix. The section is supported on a ZnS optical window glued on a metal disk.

Spectromicroscopy resolution was estimated using the knife edge method.<sup>2</sup> Lines of PTIR spectra are recorded across the border between the PMMA bead and the epoxy matrix. The OPO laser was used as a light source, providing 10 ns pulses at 1 ms intervals. Spectra were recorded in the 1680 – 1780  $\text{cm}^{-1}$  range at each point using the IR peak channel and the 393 kHz cantilever resonance. The resolution of each line measurement was assessed from the area of the ester carbonyl absorption band of PMMA around 1730  $\text{cm}^{-1}$  as a function of position. The distance between the points at 20% and 80% of the edge total height was used as an estimate of resolution. Spectra were collected in 30 nm steps. The same feedback loop parameters and setpoint are retained throughout all spectra from the same plot. The average resolution value measured over three spectromicroscopy experiments is 160 nm.

## *S3. Depth response in conventional PTIR.*

The depth response of a photothermal measurement, i.e. the depth of the surface layer from which most of the photothermal generated signal is generated, is described by the thermal diffusion length,  $L$ , and is typically estimated using equation S1, assuming that the sample is a homogeneous material of thickness much greater than  $L$ .  $f$  is the light pulsing frequency and  $\alpha$  is the thermal diffusion coefficient. Non-linearity in the Grüneisen parameter of the sample material may lead to much smaller values of  $L$  when using pulsed excitation, provided that the sample is not allowed to fully thermalize after each pulse. However, this condition requires longer pulses, of the order of 100 ns or more, and shorter pulse spacing, of the order of 10  $\mu\text{s}$  or less.<sup>1</sup> Non-resonant PTIR in the present work uses 10 ns pulses at 1 ms interval, thus ensuring full thermalization, as already demonstrated.<sup>3</sup> For a polymer or other soft matter,  $\alpha$  is of the order of 0.001  $\text{cm}^2/\text{s}$  and it follows from Equation S1 that  $L$  is of the order of 5  $\mu\text{m}$ , larger than an adherent cellular sample.

$$L = \sqrt{\frac{\alpha}{\pi f}} \quad (\text{S1})$$

*Equation S1. Thermal diffusion length of a thermal wave from the surface of an absorbing region.  $L$ , thermal diffusion length.  $f$ , light pulsing frequency.  $\alpha$ , thermal diffusion coefficient.*

#### S4. Photothermal Temperature Increase.

We can estimate an upper limit of the temperature increase induced by the photothermal effect ( $\Delta T$ ) in the absorbing location by using the following quantities.

$\mu$ : absorption coefficient ( $\text{m}^{-1}$ )

F: fluence ( $\text{J}\cdot\text{m}^{-2}$ )

$c_v$ : specific heat at constant volume ( $\text{J}\cdot\text{Kg}^{-1}\cdot\text{K}^{-1}$ )

$\rho$ : density ( $\text{Kg}\cdot\text{m}^{-3}$ )

$\eta$ : energy conversion efficiency (from vibrational excitation to internal energy)

If we assume that all photons are absorbed within one unit of the absorption coefficient, we can use equation S2 as an upper estimate of  $\Delta T$ :

$$\Delta T = \eta \frac{\mu F}{\rho c_v} \quad (\text{S2})$$

If we also assume  $\eta \sim 1$ , we set another upper limit to the temperature increase and the pressure increase from photothermal excitation.

The quantities used in Equations S3 are available for PMMA<sup>4</sup> and we can use them to estimate the maximum  $\Delta T$  for the case of excitation in the C-H bond stretching region.

$$\mu_{2860 \text{ cm}^{-1}} = 3.5 \times 10^{-4} \text{ (m}^{-1}\text{)}$$

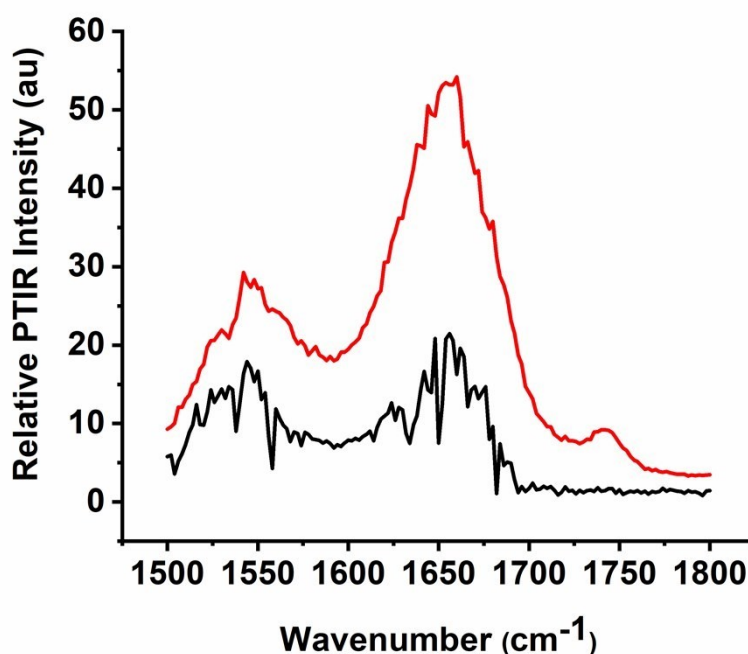
$$c_v = 1.5 \times 10^2 \text{ (J}\cdot\text{Kg}^{-1}\cdot\text{K}^{-1}\text{)}$$

$$\rho = 1.2 \times 10^3 \text{ (Kg}\cdot\text{m}^{-3}\text{)}$$

For laser power equal to 0.5 mW (a typical power level for these experiments of Figure 2), pulse duration of 10 ns, and size of the laser spot equal to  $10^4 \mu\text{m}^2$ , we have a maximum value of fluence  $F = 5 \times 10^{-5} \text{ J}\cdot\text{m}^{-2}$ . It follows that  $\Delta T \approx 0.01 \text{ K}$  for one pulse. Assuming no heat dissipation for the duration of the pulse and between pulses (setting another maximum limit), 10 to 100 pulses add up to give  $\Delta T \approx 0.1 - 1.0 \text{ K}$  for the measurement of one spectral or spatial point. While the approximations used to obtain this estimate are crude, they define an upper limit for the temperature increase obtained in these experiments. These values of  $\Delta T$  are tolerable to most cellular samples. However, it is important to note that higher laser powers and samples with higher absorption coefficient at the specific wavelength of interest can lead to much higher values of  $\Delta T$ .  $\Delta T$  values can range from 1 mK to a 100 K and care must be taken to assess the appropriate conditions for each experiment, including the possibility for the sample to dissipate heat to the surrounding environment.

### S5. Comparison of spectra

Supporting Figure S2 compares one non-resonant and one resonant PTIR spectrum, extracted from Figure 2 and Figure 5 of the main text, respectively. The intensity of the non-resonant spectrum has been decreased by dividing by a factor of 10 to facilitate comparison. The resonant spectrum displays a higher contribution from atmospheric water vapor absorption. At least part of the contribution could arise from an incomplete correction of the intracavity-enhanced absorption from water vapor in the QCL, which is not purged, although additional effects are also likely to be present. In addition, the resonant spectrum displays higher noise levels, evident in the spectral region above 1700  $\text{cm}^{-1}$ . The source of the higher noise levels deserves further investigation, but it is tentatively attributed to the contribution from the thermal noise of the specific cantilever resonance in use, which is absent in non-resonant



operation.<sup>5</sup>

**Supporting Figure S2. Comparison of non-resonant and resonant PTIR spectra.** Red Line: Non-resonant PTIR cellular spectrum from Figure 2 of the main text. Black Line: resonant PTIR cellular spectrum from Figure 5 of the main text.

### S6. References for Supporting Information

- 1 L. Quaroni, *Anal. Chem.*, 2020, **92**, 3544–3554.
- 2 E. Levenson, P. Lerch and M. C. Martin, *Infrared Phys. Technol.*, 2006, **49**, 45–52.
- 3 A. M. Katzenmeyer, G. Holland, J. Chae, A. Band, K. Kjoller and A. Centrone, *Nanoscale*, 2015, **7**, 17637–17641.
- 4 A. N. Morozovska, E. A. Eliseev, N. Borodinov, O. S. Ovchinnikova, N. V. Morozovsky and S. V. Kalinin, *Appl. Phys. Lett.*, 2018, **112**, 033105.

- 5 M. D. Frogley, I. Lekkas, C. S. Kelley and G. Cinque, *Infrared Phys. Technol.*, 2020, **105**, 103238.